*Annals of Glaciology*

# Tracing the rapid loss of Breifonn, Norway's southernmost glacier

Liss Marie Andreassen[1], Benjamin Robson[2,3], Mark Smith[4], Paul Weber[1], Jonathan L. Carrivick[4] and Bjarne Kjollmoen[1]

[1]Section for Glaciers, Ice and Snow, Norwegian Water Resources and Energy Directorate (NVE), Oslo, Norway; [2]Department of Earth Science, University of Bergen, Bergen, Norway; [3]Bjerknes Centre for Climate Research, Bergen, Norway and [4]School of Geography and water@leeds, University of Leeds, Leeds, UK

**Letter**

**Cite this article:** Andreassen LM, Robson B, Smith M, Weber P, Carrivick JL, Kjollmoen B (2025) Tracing the rapid loss of Breifonn, Norway's southernmost glacier. *Annals of Glaciology* **66**, e30, 1–9. https://doi.org/10.1017/aog.2025.10029

Received: 2 June 2025
Revised: 28 October 2025
Accepted: 30 October 2025

**Keywords:**
glacier; orthophotos; satellite; Sentinel-2; snow; vanishing

**Corresponding author:**
Liss Marie Andreassen;
Email: lma@nve.no

## Abstract

Global climate change is causing glaciers to shrink, and in some cases, to vanish completely. Glaciers in Norway are no exception. Glacier inventories, archived imagery and topographic maps across Norway help trace the decadal evolution of individual glaciers. This study focuses on Breifonn (59.75°N, 6.89°E), the southernmost glacier in Norway. Using photogrammetric analyses of historical aerial photography, satellite data and uncrewed aerial vehicle data, we quantify how Breifonn has changed from its 'pre-industrial' Little Ice Age extent to its present size. Our geomorphology-based glacier reconstruction indicates that Breifonn covered an area of $5.8 \pm 1.2$ km$^2$ during the Little Ice Age. Its main part reduced in area from $3.3 \pm 0.3$ km$^2$ in 1955 to $0.17 \pm 0.02$ km$^2$ in 2024 (94%) and has thinned on average by $0.4 \pm 0.02$ m a$^{-1}$ between 1978 and 2019. Since the 1980s, the glacier has fragmented into several disconnected ice bodies. If current melt rates persist, Breifonn may disappear entirely soon.

## 1. Introduction

Mountain glaciers are at risk of extinction, which is complete disappearance, due to global climate change. The imbalance between the current climate and glacier geometry varies greatly between regions. Scandinavia is a region projected to experience substantial losses regardless of the degree of future warming (Zekollari and others, 2025). The consequences of losing mountain glaciers span biodiversity loss, tourism decline, impacts on societal health and livelihood, and cultural heritage (e.g. Purdie, 2013; Ezzat and others, 2025; Burrill and others, 2025; Howe and Boyer, 2025).

Norwegian glaciers span a wide geographical range from the northernmost glaciers at 70° North in Finnmark County to the southernmost glaciers at 59° North in Rogaland County (Andreassen and others, 2012). Norway has a rich record of glaciological and geodetic mass balance observations, as well as frontal variation measurements on many glaciers (Andreassen and others, 2020). However, most glaciers lack field observations and have only been studied through repeat glacier inventories (e.g. Østrem and others, 1969; 1988), which limits the depth and scope of possible analysis. An increasing number of historical aerial photographs are being scanned and made available through the Norwegian Mapping Authority's web portal, *Norgeibilder.no* as orthophotos. These datasets offer higher spatial resolution for analysis and allow for interpretations predating the satellite era. A comparison of orthophotos from 1978 with the most recent 2019 glacier inventory revealed that Breifonn has greatly reduced in area over the 41 year period (Andreassen, 2022). Breifonn was therefore included in the Global Glacier Casualty List (GCCL) launched in August 2024 (Boyer and Howe, 2024). The GCCL is a platform dedicated to documenting and commemorating glaciers that have disappeared or soon-to-disappear due to climate change (Raup and others, 2025).

In this paper, we document changes in the area of Breifonn from its 'pre-industrial' Little Ice Age (LIA) extent to 2024, using geomorphological mapping, glacier inventories, historical maps, aerial photographs and recent satellite imagery. We derive digital terrain models (DTMs) from historical photos from 1955 and 1978 and make a new DTM from our own survey using Uncrewed Aerial Vehicle (UAV) during a field visit to the glacier in August 2024 to assess elevation changes and geodetic mass balance. We also assess the associated methodological uncertainties, which arise primarily from limited geomorphological evidence and challenges in delineating glacier outlines and reconstructing Breifonn's ice surface topography due to persistent snow cover. Our aim is to document the profound changes the glacier has undergone over the industrial period and discuss whether Breifonn can still be considered a glacier.





https://doi.org/10.1017/aog.2025.10029 Published online by Cambridge University Press

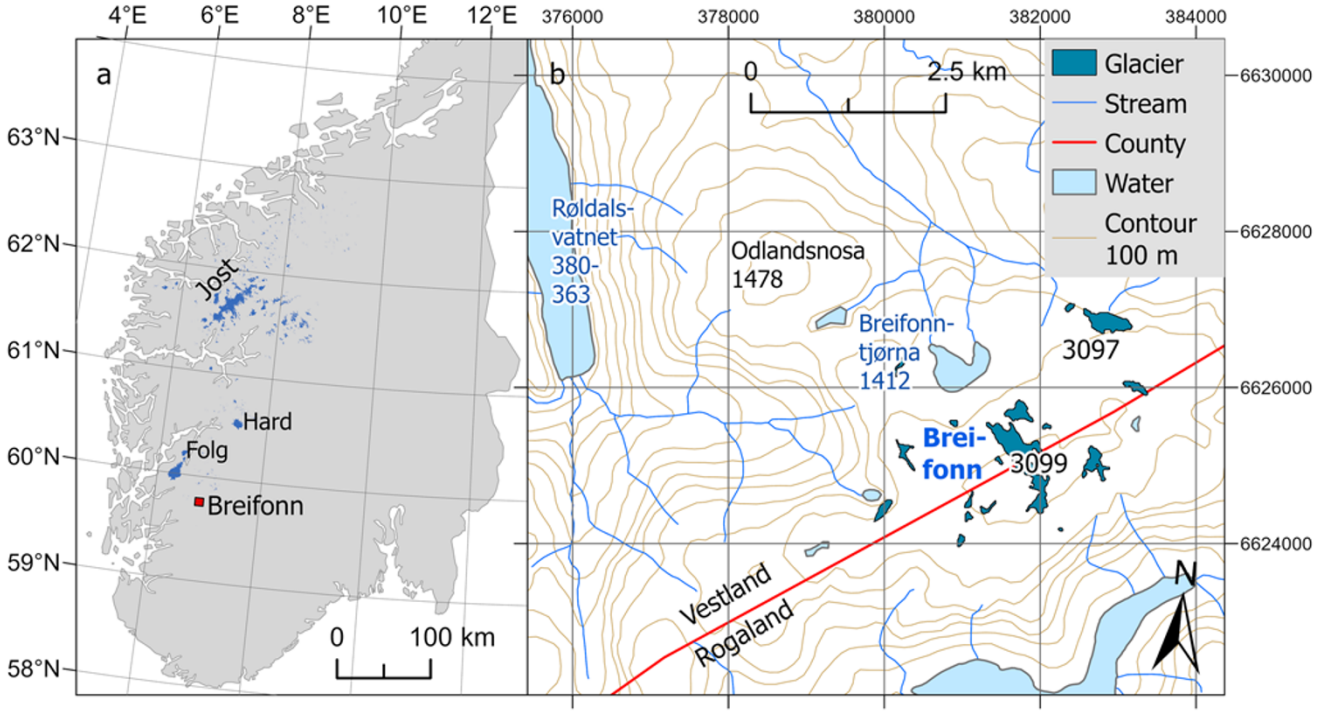


**Figure 1.** Location map showing (a) Breifonn in southern Norway, south of the largest glaciers Folgefonna, Hardangerjøkulen and Jostedalsbreen, and (b) Breifonn on the border between the counties Vestland and Rogaland. The glacier outlines and selected glacier IDs (3097 and 3099) are from 2019 (Andreassen and others, 2022). Coordinates are geographical (a) and UTM Zone 32 N (b).

## 2. Setting

Breifonn (59.75°N, 6.89°E) is a small glacier on the border between Rogaland and Vestland counties (Fig. 1). It is the southernmost glacier in Norway and has been included in all the published glacier inventories of southern Norway (Liestøl, 1962; Østrem and others, 1969; 1988; Andreassen and others, 2012; Winsvold and others, 2014; Andreassen and others, 2022). Some ice bodies further south were included in the recent glacier inventories, but since they were smaller than 0.1 km$^2$ they were categorised as snow or ice patches (Andreassen and others, 2012; Andreassen, 2022). Breifonn has also been spelt as Breidfonn, Bredfond and Breifond on historical maps. To our knowledge, no glaciological investigations of Breifonn exist beyond the national glacier inventories.

Information on Breifonn's extent and evolution prior to the 1950s is sparse and fragmented. Southern Norwegian glaciers generally advanced to more extended positions during the LIA (Grove, 2004), offering a useful proxy for their 'pre-industrial' state. Although there is no direct dating of Breifonn's LIA advance, data from the nearby Folgefonna ice cap suggest a maximum LIA extent between the 1870s (Nussbaumer and others, 2011) and the 1930s (Tvede, 1973). On historical maps, Breifonn appears in full only on a hand-drawn portfolio map sheet (*porteføljekart*) by Staib (1860), part of Norway's main map series produced between approximately 1817 and the 1860s (Harsson and Aanrud, 2016). The section of the map featuring Breifonn is based on field surveys carried out in 1856–57, documented in two rectangular survey maps (*rektangelmålinger*) by Scharffenberg (1856) and Naeser (1857). In these maps, Breifonn is shown as covering substantial portions of the plateau summit. Several adjacent mountain plateaus appear similarly covered, as indicated by the distinctive turquoise colouration used for these summit areas. The accompanying field survey reports, which provide detailed topographic descriptions of the mapped area, refer to these summits as '*sneefjelder*' ('mountains covered with snow year-round'). This suggests that most of these features likely represented mountain plateaus covered with perennial snowfields, rather than actual ice masses. Mountaineers' accounts in Norwegian Tourist Association yearbooks provide early 20th-century descriptions and photographs of the glacier (Wareberg, 1927; Johannessen, 1928; Anda and Sagen, 1941). Johannessen (1928) dubbed Breifonn 'Norway's South Pole' and claimed an area of 30 km$^2$, likely an overestimate influenced by the exceptionally cold summer and widespread snow that year. Anda and Sagen (1941) describe Breifonn as a 'gently curved shield […], blending seamlessly into the surrounding landscape without any abrupt drop' (p. 99; translated from Norwegian), with a smooth, crevasse-free surface.

Breifonn is located west of the main water divide in an area of high precipitation in southwestern Norway. It has an annual precipitation of about 2000 mm and a mean annual air temperature of −2.5°C (estimated for 1579 m a.s.l.) for the reference period 1991–2020 (SeNorge, 2025). In 2003, Breifonn spanned an elevation range from 1417 to 1601 m asl, with a slope of 7 degrees and a north-facing aspect (Andreassen and others, 2012). The bedrock of the plateau summit on which Breifonn rests is composed of mica gneiss (Sigmond, 1975).

## 3. Data and methods

### 3.1. Glacier inventories

All published glacier inventories of southern Norway/Norway have included area estimates on Breifonn. In the following, we detail the information and sources used. In the first 'List of areas and

https://doi.org/10.1017/aog.2025.10029 Published online by Cambridge University Press

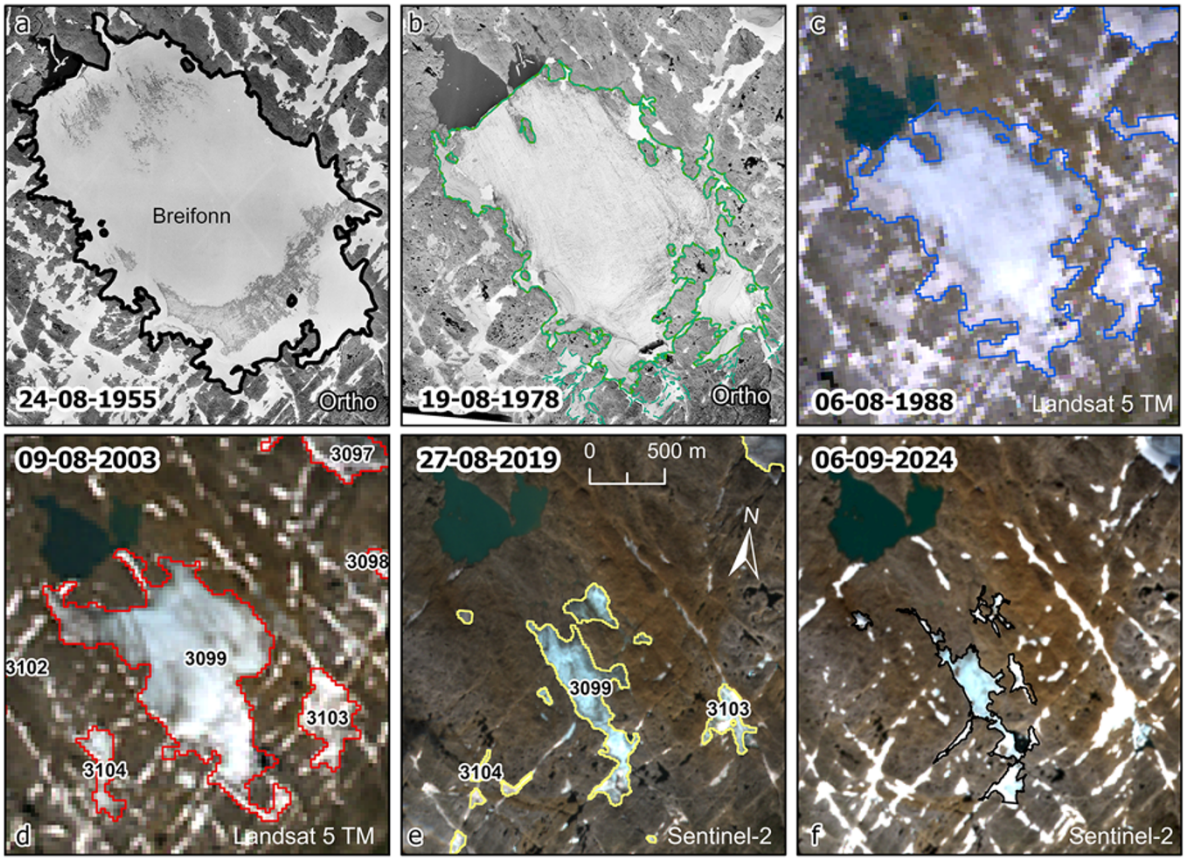


**Figure 2.** The demise of Breifonn from 1955 to 2024 was displayed using orthophotos (Ortho) and Satellite imagery (Landsat 5 TM and Sentinel-2). All outlines are from the year of mapping. Note the lake in the upper left corner that has emerged as the glacier has now retreated from it.

numbers of glaciers', Breifonn is listed with an area of 3.2 km$^2$ with reference to 1955 (p. 50, Liestøl, 1962). The same images or map were used in the first inventory of glaciers in South Norway (Østrem and Ziegler, 1969), in which Breifonn is divided into two parts, units 7 and 8. The northwestern part has an area of 2.65 km$^2$, whereas the part facing southeast has an area of 0.64 km$^2$, totalling 3.27 km$^2$. In the inventory of South Norway published in 1988, Breifonn is listed as Breidfonn, as one unit, with an area of 2.61 km$^2$ (Østrem and others, 1988). None of these inventories is available with digital outlines, only tabular data. Digital outlines exist from a Landsat 1988–97 glacier inventory (Winsvold and others, 2014). Here, Breifonn is mapped from a Landsat 5 TM 1988 image, and the area of the main part is 1.91 km$^2$ (Fig. 2c). Breifonn is also covered using a Landsat 5 TM scene of 9 August 2003 (Andreassen and others, 2012). Breifonn is listed with ID 3099 and with several small units around it (Fig. 2d). The area of Breifonn (3099) is listed as 1.37 km$^2$. In the latest inventory made using Sentinel-2 imagery, the image covering Breifonn was taken on 27 August 2019; the glacier had disintegrated in several parts (Fig. 2e) with the largest remaining part (3099) having a size of just 0.26 km$^2$ (Andreassen, 2022).

Another digital dataset that digitised glacier outlines from first-edition 1:50,000 topographical maps in the N50 series from the Norwegian Mapping Authority (Winsvold and others, 2014). Breifonn was in that study digitised from the N50 sheets 1314-1 Røldal and 1314-2 Suldalsvatnet that were based on aerial photographs acquired in 1953, 1955 and 1961. Likely it is the 1955 photos used for the part covering Breifonn. The outline on the maps is patchy and seemingly includes many snowfields (Fig. 3b). The total area of the continuous part of Breifonn in the N50 product is 5.5 km$^2$.

### 3.2. Aerial photos

Several aerial photos of Breifonn exist for the period 1955–2019, but not all are available digitally from the Norwegian Mapping Authority's web portal *Norgeibilder.no* as orthophotos. All orthophotos available from *Norgeibilder.no* were checked as part of this study. Many of the orthophotos are from a time of severe snow conditions and so are not optimal for assessing glacier extent or condition. In the photos from 1981, 2012 and 2013, the glacier and surroundings were almost fully snow-covered; in the photos from 1955, most of the glacier was snow-covered (Fig. 2a), whereas the images from 1978 (Fig. 2b) and 2019 (not shown) had the best/least snow conditions. We therefore ordered the 1955 and 1978 photos as individual photos from the Norwegian mapping authorities for further data processing to generate DTMs and derive elevation changes, and compute geodetic mass balances.

### 3.3. Digital terrain models

We constructed several new DTMs for this study using a DTM from 2019 from the Norwegian Mapping Authority as a reference. In the following, we describe each DTM.

https://doi.org/10.1017/aog.2025.10029 Published online by Cambridge University Press

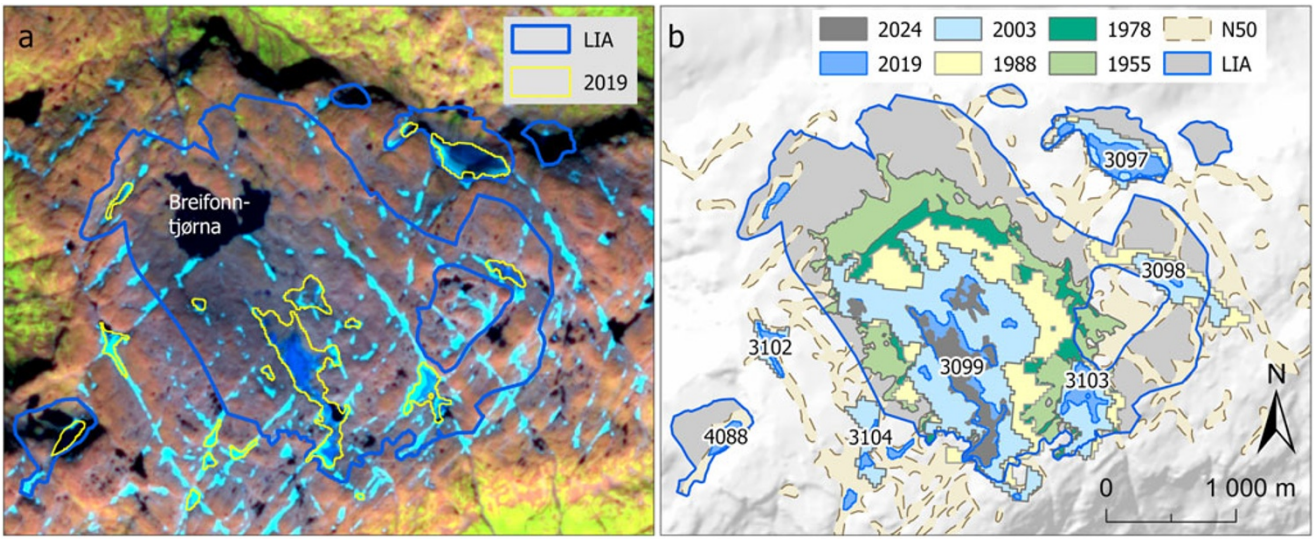


**Figure 3.** Glacier outlines of Breifonn from the 'pre-industrial' LIA to 2024. (a) LIA and 2019 outlines shown with a Sentinel-2 satellite image in false colours from 6 September 2024 (Copernicus Sentinel data). The dark grey-brownish zone (in the centre of the figure) southeast of the Breifonntjørna lake is interpreted as the footprint left by glacial coverage during the LIA. (b) Outlines shown as coloured polygons with a terrain shadow as background (Norwegian Mapping Authority). The 2024 outline was manually digitised from UAV orthophoto (Figure 4b).

#### 3.3.1. 2019

A photogrammetry-derived point cloud, as well as 1 and 10 m DTMs, is available from the Norwegian Mapping Authority based on the 2019 aerial photographs. The exact acquisition dates of the 2019 survey are not known, as the images were taken over a range of days. The 2019 DTM at 1 m resolution was used as a reference for other DTMs in this work. No airborne laser scanning is available for this region.

#### 3.3.2. 1955 and 1978

Aerial imagery from both 1955 (five images, mean altitude 3690 m a.s.l.) and 1978 (five images, mean altitude 2430 m a.s.l.) was aligned using Structure-from-Motion (SfM) photography in Agisoft Metashape. Camera calibration reports were not available, so the camera's mathematical model was reconstructed by identifying the fiducial markers in each image and subsequently using automatically collected tie points between the images. In the absence of any control point data for the historical images, they were initially aligned in an arbitrary coordinate system, but then georeferenced to manually-identified relatively fixed points (e.g. large bedrock features) using the 2019 orthoimagery and accompanying elevation model for reference. Using these coordinates as manual Ground Control Points (GCPs), the 1978 model was aligned using the nine GCPs with a mean RMS error of 2.34 m. The same process was followed for the 1955 images using eleven GCPs with an RMS error of 2.40 m. DTMs were generated without interpolation to ensure only valid image matches were used in the DTM differencing. DTMs for the 1955 and 1978 surveys were exported at 1 m resolution, while orthomosaics were exported at 0.4 and 0.2 m in 1955 and 1978, respectively.

#### 3.3.3. 2024 UAV

On 28 August 2024, we conducted a UAV-based SfM photogrammetry field survey covering the extent of the Breifonn glacier to provide an updated and high-resolution assessment of the extent and to construct a DTM (Smith and others, 2016). Aerial imagery was acquired using a DJI Mavic 3 Enterprise UAV. Ground control was unavailable during the field survey; however, the imagery was directly georeferenced using a real-time kinematic positioning (RTK) module communicating with a DJI D-RTK 2 high-precision real-time kinematic positioning (GNSS) receiver acting as a base station, located at the ice margin. While not as accurate as an independent GNSS survey of GCPs located within the study area (James and others, 2017), the centimetre-level positioning was deemed sufficient for these mapping purposes, and the relatively lightweight field equipment was more optimal for a remote field location. In total, 363 images were collected from manual flight lines with a minimum 80% sidelap and 60% frontlap between successive images. Additional off-nadir images were taken along flight lines to minimise any doming effects arising in the image alignment process.

SfM photogrammetry was performed using Agisoft Metashape (version 2.0.2) following the workflow of James and others (2017). The mean image location accuracy was $<0.02$ m. In total, 347 images aligned successfully, with a 3D root mean square (RMS) error of 0.068 m. Dense point clouds were created and rasterised to produce a 0.227 m resolution DTM. An orthomosaic image was created at 0.0057 m resolution. Both data products were exported in the ETRS 1989 UTM Zone 32 N coordinate system. Errors are well constrained within the glacier outline that was the focus of the field survey and used to calculate glacier geometry; however, errors will be larger on the ice-free surfaces outside of this region.

### 3.4. Glacier outline delineation and LIA reconstruction

Glacier outlines were digitised from orthophotos from 1955, 1978, 2019 and 2024. The existing N50 outline digitised from the topographic maps was very patchy (Fig. 3b). Most of the glacier was snow-covered, and the outline digitised at the time of mapping likely mapped both snow and ice. The 1955 outline was derived using the N50 outline as reference and edited to fit the 1955 orthophoto excluding many of the likely snowfields (Fig. 2a). The 1978 outline was already digitised from orthophoto (Andreassen,

https://doi.org/10.1017/aog.2025.10029 Published online by Cambridge University Press

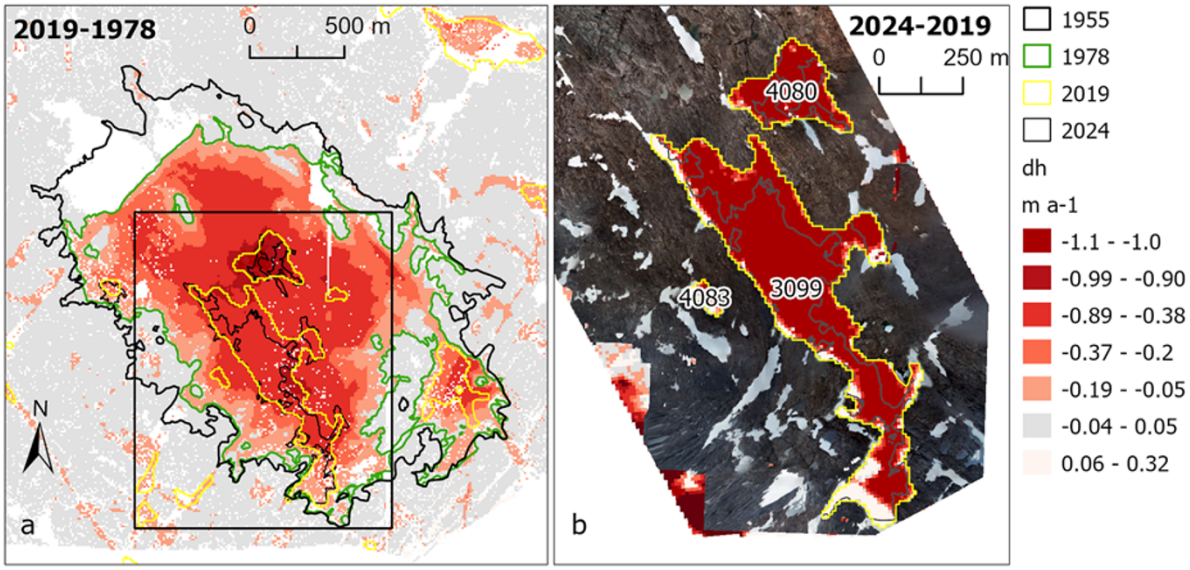


**Figure 4.** Elevation change (m $a^{-1}$) for Breifonn from 1978 to 2019 and 2019 to 2024. Background orthophoto in (b) is from the UAV survey of 28 August 2024. Note the difference in scale, the box in (a) is the extent of (b).

2022) and here edited slightly by removing some of the patchy outlines in the southern part (Fig. 2b). We also used the DTM differencing results to aid the outline editing. The 1988, 2003 and 2019 outlines from satellite imagery were used without modifications. These outlines were derived using a semi-automated method from satellite images (Andreassen and others, 2012, 2022; Winsvold and others, 2014). The 2024 outline was manually digitised from the UAV orthophoto covering the main part of the present glacier (Fig. 4b).

We estimated Breifonn's 'pre-industrial' LIA glacier extent by adopting an approach used elsewhere in Norway, including for Jotunheimen (Baumann and others, 2009), Hardangerjøkulen (Weber and others, 2019), Langfjordjøkelen (Weber and others, 2020) and Jostedalsbreen (Carrivick and others, 2022). This approach involved the visual interpretation of aerial photographs available in ArcGIS Pro base images, Norgeibilder (with the 2019 imagery also available as colour-infrared imagery) and a hill-shaded image of the 2019 DTM to identify glacial landforms around Breifonn. Specifically, the landforms identified were predominantly glacial lineations (grooves or ridges formed by glacier movement, showing ice flow direction), erosional boundaries (the transition between recently ice-moulded bedrock and more weathered and/or lichen-covered bedrock), glacial drift limits (the boundary between terrain covered by glacially transported sediments and adjacent surfaces of different composition or older glacial drift), as well as ice-marginal moraines (ridges deposited at the glacier margin). Typically, landforms and glacial drift deposits relating to the LIA appear relatively fresh, clean, unvegetated, unweathered and uncolonised by lichen. Mapping of LIA glacial landforms was further directed by the historical glacier inventories, and a field visit in August 2024 was used to inform some of the mapping. The rather vague, disparate (and undated) erosional and drift boundaries, as well as ice-marginal moraines, were joined to create a continuous glacier outline for the LIA. This outline is a best guess, digitised from one glacial landform to the next, following topography logically.

The satellite-derived glacier inventories have an estimated overall area uncertainty of ± 3%, but with larger relative uncertainties for smaller glaciers (Andreassen and others, 2012, 2022; Winsvold and others, 2014). Due to Breifonn's smaller size and uncertainties related to snow around the perimeter, we therefore estimate an area uncertainty of ± 10% for the satellite-derived outlines (1988, 2003, 2019) as well as the orthophoto-derived outlines (1955, 1978, 2024). As noted by Paul (2013), the precision of the derived glacier area is not necessarily higher when using high-resolution data. In the case of Breifonn, the snow-covered parts cause the greatest uncertainty. For the reconstructed LIA glacier extent, we estimate a relative area uncertainty of 20%. This is based on the studies by Carrivick and others (2022) and Reinthaler and Paul (2023), who both consider uncertainty from subjective interpretation of geomorphological features and from variability in digitising glacier outlines.

### 3.5. DTM differencing

The DTMs from 1955, 1978, 2019 and 2024 were co-registered and differenced using the XDEM Python library (Hugonnet and others, 2024). For each successive DTM pair, the older elevation model was co-registered relative to the more recent elevation model (except for the 2024 model, which was co-registered against the 2019 dataset). Non-linear co-registration biases were corrected using an Iterative Closest Point alignment, which can account for rotations between datasets. Subsequently, we followed the method set out by Nuth and Kääb (2011), which seeks to minimise the RMSE slope normalised elevation biases over stable terrain to solve sub-pixel linear alignments. The co-registration shifts are summarised in Table S1.

The resulting elevation change rasters had voids over areas with low image contrast, such as fresh snow or shadows. These voids were filled using a third-order polynomial hypsometric binning approach (after McNabb and others, 2019) with a bin size of 10 m. It was deemed that the voids on the 1955 DTM, however, were too substantial to fill, and as such this DTM was used only for comparing thinning rates within the small part (9.5%) covered.

https://doi.org/10.1017/aog.2025.10029 Published online by Cambridge University Press

**Table 1** Area changes of Breifonn from published data and produced in this study. The 1955 outline is used as a reference after the breakup of Breifonn into the main glacier part (ID 3099) and other fragmented parts (other) after 1978. AP, aerial photos; map, topographical map; LIA, Little Ice Age maximum extent. Area estimates are reported with a ± 10% uncertainty range for outlines derived in this work, except for the LIA outline, which we estimate to 20%; see main text for details.

| Year | Area (km$^2$) | ID 3099 (km$^2$) | Other (km$^2$) | Source | Reference |
|---|---|---|---|---|---|
| LIA | 5.79 ± 1.2 | – | – | Geomorphological reconstruction | This work |
| 1955 | 3.20 | – | – | aP map | Liestøl, 1962 |
| 1955 | 3.27 | – | – | aP map | Østrem and Ziegler, 1969 |
| 1955 | 3.33 ± 0.33 | – | – | aP | This work, digitised from orthophoto |
| 1978 | 2.38 ± 0.24 | – | – | aP | This work |
| 1981 | 2.61 | – | – | aP | Østrem and others, 1988 |
| 1988 | 2.11 ± 0.21 | 1.91 ± 0.19 | 0.20 ± 0.02 | Landsat 5 TM | Winsvold and others, 2014 |
| 2003 | 1.56 ± 0.16 | 1.37 ± 0.14 | 0.19 ± 0.02 | Landsat 5 TM | Andreassen and others, 2012 |
| 2019 | 0.39 ± 0.04 | 0.26 ± 0.03 | 0.13 ± 0.01 | Sentinel-2 | Andreassen and others, 2022 |
| 2024 | 0.22 ± 0.02 | 0.17 ± 0.02 | 0.05 ± 0.01 | aP UAV | This work |

We calculated the geodetic mass balance, $B_{geod}$:

$$B_{geod} = \Delta V \times f_{\Delta V}/A \quad (1)$$

where A is the average glacier area of the two surveys, assuming a linear change in time, and ΔV is the volume change. We applied a density conversion factor, $f_{\Delta V}$, of 850 ± 60 kg m$^{-3}$ (Huss, 2013). Glacier elevation-change uncertainty was estimated with the xDEM implementation of Hugonnet and others (2022), which models heteroscedastic, spatially correlated errors via variograms from stable terrain and terrain slope/curvature, producing gridded error fields. These spatial errors were propagated and combined with the density conversion term and a 10% area uncertainty to obtain the total geodetic mass-balance uncertainty.

## 4. Results

### 4.1. Area change

Our LIA reconstruction indicates that the 'pre-industrial' glacier extent of Breifonn was 5.8 ± 1.2 km$^2$ (Table 1). Breifonn was covering the bowl-shaped central part of the plateau summit area, including the area now occupied by the Breifonntjørna lake (Fig. 3a). The terrain surface in this area is ice-moulded and draped with a thin layer of fresh-looking glacial drift that is densely streamlined and fluted, providing strong evidence of recent LIA glacial coverage. This glacial imprint is readily identifiable in the 2019 aerial imagery as a brownish, rust-coloured zone that contrasts sharply with the surrounding greyish terrain. In the Sentinel-2 imagery shown in Figure 3a, this area appears as a darker grey-brownish zone, clearly distinct from the lighter brownish surroundings. However, the transition between these two zones is often indistinct and diffuse, making it challenging to pinpoint and map the exact location of erosional and drift boundaries. This introduces some degree of uncertainty regarding the lateral and frontal positions of the reconstructed LIA glacier margin. Areas of the plateau summit lying outside this zone are largely clean, lacking lichen colonisation, and exhibit a grey, almost 'bleached' appearance. This suggests that these plateau summit surfaces remained permanently snow-covered during the LIA. Furthermore, our reconstruction indicates the presence of five very small cirque glaciers along the plateau edges, with a combined area of approximately 0.7 ± 0.2 km$^2$. Of these, glacier ID 3097 is included in the N50, 1988, 2003 and 2019 inventories, while glacier ID 4088 appears only in N50 and 2019 inventories (Fig. 3b).

In 1955, the area of Breifonn was 3.3 ± 0.3 km$^2$, and in 2024, the area of the largest remaining part was only 0.17 ± 0.02 km$^2$. Counting all glacier parts within the 1955 outline shows a reduction in glacier area from 3.3 ± 0.3 to 0.22 ± 0.02 km$^2$ in the period 1955–2024, resulting in an overall area reduction of 93% or 1.4% a$^{-1}$ over the 69 years. The orthophotos and satellite imagery show that Breifonn split into several parts between 1978 and 1988 (Figs. 2b,c and 3b).

### 4.2. Elevation change and geodetic mass balance

The DTM differencing shows that Breifonn has thinned continuously over all time periods studied. Between 1978 and 2019 (41 years), the glacier thinned by an average of −0.40 ± 0.02 m a$^{-1}$, with the largest thinning occurring at the centre of the glacier, with a total thinning of up to 45 m (Fig. 4). The geodetic mass balance over the 1978–2019 period is −0.58 ± 0.07 m w.e. a$^{-1}$. Over the last period 2019–24 (5 years), the main remnants of Breifonn (ID 3099 and 4080) experienced average thinning of 0.75 ± 0.11 and 0.90 ± 0.15 m a$^{-1}$, respectively, with maximum thinning of nearly 12 m over the five-year period. The two other smaller parts (4081 and 4083) covered by the 2024 survey showed less thinning of 0.10 ± 0.16 and 0.03 ± 0.16 m a$^{-1}$, respectively. The geodetic mass balance of Breifonn (3099) in the 2019–24 period is −0.78 ± 0.25 m w.e. a$^{-1}$. As mentioned, we were not able to derive a glacier-wide estimate for 1955–78 due to significant voids in the 1955 DTM. For the portion of the DTM that had elevation values, the glacier thinned on average by 0.77 ± 0.09 m a$^{-1}$ between 1955 and 1978. Given that the accumulation area was not covered, these values are not considered representative of the entire glacier.

## 5. Discussion

### 5.1. Factors influencing area estimates

As the glacier outlines of Breifonn are partly covered in snow, the interpretation of snow fields influences the resulting areas and area changes. For instance, the area was greatly reduced by using the 1955 orthophoto instead of the N50 outlines, from 5.5 to 3.3 km$^2$. Our estimate is, however, similar to the glacier inventories of Liestøl (1962) and Østrem and others (1969) using the same photos. Furthermore, small edits of the southern part of the 1978 extent of Breifonn reduced the area from 2.51 to 2.38 km$^2$, a difference of 5% showing that the area will vary depending on human interpretation of orthophotos in line with previous studies (e.g. Paul and others, 2013). Two orthophotos of Breifonn in 2019 are available on Norgeibilder.no. One from 26 July 2019 has several snow fields resulting in an area of 0.58 km$^2$ for the biggest part (3099) when including these in the outline. The one from 21 September 2019 is fully covered in a fresh layer of snow and was therefore not used for area estimates. The Sentinel-2 outline we use for our calculations gives an area of 0.26 km$^2$ for

https://doi.org/10.1017/aog.2025.10029 Published online by Cambridge University Press


**Figure 5.** Photographs of Breifonn showing (a) a historical view of the glacier and its surroundings from afar, taken between 1947 and 1949 (Owner: Nasjonalbiblioteket); (b) the middle section of the present-day glacier; (c) one of its detached parts. Both (b) and (c) were taken on 28 August 2024 by Liss M. Andreassen.

Breifonn on 27 August 2019. This emphasises the need for checking sources and selecting orthophotos or satellite data with little seasonal snow cover if available. In the case of Breifonn and many other glaciers in Norway, cloud conditions and seasonal snow are the main hindrances to obtaining accurate data (e.g. Paul and others, 2011).

The reconstructed LIA outline represents our best estimate, with accuracy constrained by limited and subdued landform evidence. Geomorphology-based LIA reconstructions are most effective where glaciers left abundant landforms, typically latero-frontal moraines and trimlines (e.g. Osipov and Osipova, 2019; Lee and others, 2021). In such cases, LIA extents are delineated by extending modern outlines down-glacier, following trimlines to the outermost LIA moraine limit (e.g. Carrivick and others, 2020; Tielidze and others, 2025). Up-glacier sections are often left unmodified, either assuming negligible post-LIA change in accumulation areas or because cirque- and valley-type glaciers are topographically confined (e.g. Stokes and others, 2018; Reinthaler and Paul, 2023; Zhang and others, 2024). In contrast, Breifonn's unconstrained plateau setting and flat, sheet-like geometry required reconstruction around its entire perimeter, not only down-glacier. Given the limited geomorphological evidence at Breifonn, the ± 20% area uncertainty we estimated may represent a lower bound, as interpretation uncertainty dominates the total error (Reinthaler and Paul, 2023). Nevertheless, the availability of a wide range of high-resolution remote sensing datasets allowed us to map the subtle features at Breifonn and so reduce uncertainties related to landform visibility.

### 5.2. Breifonn's classification as a glacier

In this paper, we document the rapid shrinking of Breifonn. The field visit in August 2024 revealed that it now consists only of fragmented ice patches. Can we still classify Breifonn as a glacier? Definitions of glaciers vary in the literature and are used differently. Cogley and others (2011) define a glacier as a 'perennial mass of ice, and possibly firn and snow, originating on the land surface by the recrystallisation of snow or other forms of solid precipitation and showing evidence of past or present flow'. Thus, it is sufficient to have evidence of past flow according to this definition. Some studies use minimum size thresholds that can depend on the spatial resolution of data sources used for the inventories or be suitable when assessing large glacier regions. However, in regions where ice bodies are sparse, even small glaciers may be of significant interest. When mapping with high-resolution imagery (<1 m) with minimal seasonal snow cover, glaciers <0.05 km$^2$ and even <0.01 km$^2$ are readily identifiable, and using a minimum size threshold may be inappropriate (Leigh and others, 2019). To address this, Leigh and others (2019) proposed a scoring system (with a possible maximum score of 20 points) to enable the identification of very small glaciers and classify them as 'certain' (11–20 points), 'probable' (6–10 points) or 'possible' (2–5 points), perennial snow (1 point) based on the following diagnostic features indicative of glacier motion: crevasses, bergschrund, visible ice, evidence of past or present flow such as flow features and deformed stratification. This classification system follows the glacier definition of Cogley and others (2011).

The orthophotos from 1955, 1978, 2006, 2019 and 2024 reveal glacier ice and evidence of past flow. The 2019 orthophotos have the highest spatial resolution and best coverage of the recently deglaciated glacier foreland. This proglacial area has a densely fluted surface with a small number of ice-marginal moraines. With a total score of 18 out of 20 points according to the Leigh and others (2019) classification system, Breifonn can be categorised as a 'certain' glacier. The only criterion it does not meet is the bergschrund, due to its initial formation as a plateau glacier, rather than a cirque or mountain glacier. Although Breifonn appears thin and downwasting now, our results reveal that its central parts were up to 50 m thicker in 1978 and thus were thick enough for the ice to deform and flow. However, the aerial photos from 1978 reveal supraglacial drainage channels typical of less active glaciers.

The 2024 field visit revealed that both the detached parts and the ice remnants of Breifonn contained clear blue glacier ice, crevasses and evidence of past flow (Fig. 5). However, Breifonn appeared too thin to sustain any significant flow. The visit also showed that even in late summer, seasonal snow can remain around the glacier margins, making it difficult to precisely define the actual outline, and thus the area, of the ice bodies. Breifonn has diminished rapidly in recent years and is expected to continue to shrink. How long it will take to completely vanish depends on both future summer melting and winter precipitation. With current rates of retreat, it may take less than 10 years. Snow-rich years may temporarily slow the loss and prolong the survival of some of Breifonn's remnants.

Breifonn presently spans a narrow elevation range of less than 200 m. Glaciers with small elevation ranges are particularly susceptible to climate warming as they have less potential to retreat to higher elevations (Zekollari and others, 2025). In contrast to Breifonn, glacier ID 3097 appears to have experienced little change in area since its 'pre-industrial' extent (Fig. 3b). Although it has retreated from its LIA position, its cirque-like setting against a cliff face likely helps to retain its size due to snow drift, its protected location and northern exposure (Fig. S1).

https://doi.org/10.1017/aog.2025.10029 Published online by Cambridge University Press

## 6. Summary and conclusions

We document the demise of Breifonn, Norway's southernmost glacier, from its maximum LIA extent to its present (2024) state as a vanishing glacier. Ice-marginal snow covers part of the glacier perimeter in all available photographs and images of Breifonn and complicates glacier outline mapping and change assessments. Reconstructing the 'pre-industrial' LIA extent of the glacier proved challenging due to the sparsity of geomorphological evidence. Despite this, our results clearly reveal that Breifonn is rapidly shrinking and has changed from an active glacier to a vanishing glacier. From the 'pre-industrial' LIA to 1955, it nearly halved in size from about 5.8 ± 1.2 km$^2$ to 3.3 ± 0.3 km$^2$. Between 1955 and 2019, Breifonn lost more than 93% of its area and disintegrated into several smaller ice patches. As of 2024, the largest remaining part with ID 3099 measured only 0.17 ± 0.02 km$^2$. The central part of the glacier experienced surface lowering of up to ∼1 m a$^{-1}$ over the period 1978–2024. We estimate a geodetic mass balance of −0.58 ± 0.07 m w.e. a$^{-1}$ between 1978 and 2019 and −0.78 ± 0.25 m w.e. a$^{-1}$ between 2019 and 2024. Breifonn formed in a region with high winter precipitation, but the current warming is taking its toll on Breifonn. The current small altitudinal range of less than 200 m will make it very difficult for the ice remnants of Breifonn to survive much longer and may soon be reported to the GLIMS list of extinct glaciers (Raup and others, 2025).

**Supplementary material.** The supplementary material is available at https://doi.org/10.1017/aog.2025.10029.

**Data availability.** Geodetic mass balance results will be submitted to WGMS. The orthophotos from 1978 and 2019 are available at *Norgeibilder.no.* The original glacier inventory outlines from N50, 1988, 2003 and 2019 are available in the GLIMS database. The new glacier outlines from LIA, 1955, 1978 and 2024 are available from Nasjonalt Vitenarkiv (https://doi.org/10.58059/wazv-zv52).

The processed DTMs and elevation change rasters are available upon request. Scanned versions of the NVE glacier inventories are available at: https://www.nve.no/vann-og-vassdrag/vannets-kretsloep/bre/publikasjoner-publications/breatlas-glacier-inventories/. The historical photograph of Breifonn (Fig. 5a) is available from Nasjonalbiblioteket (https://urn.nb.no/URN:NBN:no-nb_digifoto_20170324_00052_NB_MIT_KNR_04218)

**Acknowledgements.** We thank two anonymous reviewers and scientific editor Etienne Berthier for valuable comments that helped us improve our manuscript. This work is a contribution to the NVE projects 'Morfologisk basert breutbredelse LIA' and 'NVE Copernicustjenester', and to the 'Klima i Norge 2100' report. Publications costs are covered by Norsk klimaservicesenter. We thank Isaac Dawson and Jenna Sutherland for assistance on the field visit to Breifonn. We are grateful to Sidsel Kvarteig (Kartverket – Norwegian Mapping Authority) for sharing her expertise on the historical maps of Breifonn and for providing access to historical survey reports.

**Author contribution.** MS and BR processed aerial photographs and digital terrain models. LMA and BK digitised glacier outlines. PW reconstructed the LIA outline. LMA and BR analysed DTM data. LMA made figures and tables. LMA wrote the manuscript with contributions from all authors. All authors commented on and contributed to the final manuscript.

## References

**Anda T and Sagen H** (1941) Breifonn fra to sider. *Stavanger Turistforening Årbok* **1941**, 98–102.

**Andreassen LM, Elvehøy H, Kjøllmoen B and Belart JMC** (2020) Glacier change in Norway since the 1960s – an overview of mass balance, area, length and surface elevation changes. *Journal of Glaciology* **66**(256), 313–328. doi:10.1017/jog.2020.10

**Andreassen LM** (2022) Breer og fonner i Norge. *NVE Rapport 3–2022*. Norwegian Water Resources and Energy Directorate. Oslo, Norway.

**Andreassen LM, Nagy T, Kjøllmoen B and Leigh JR** (2022) An inventory of Norway's glaciers and ice-marginal lakes from 2018–19 Sentinel-2 data. *Journal of Glaciology* **68**(272), 1085–1106. doi:10.1017/jog.2022.20

**Andreassen LM, Winsvold SH, Paul F and Hausberg JE** (2012) Inventory of Norwegian glaciers. *NVE Report 38-2012*. Norwegian Water Resources and Energy Directorate, Oslo, Norway.

**Baumann S, Winkler S and Andreassen LM** (2009) Mapping glaciers in Jotunheimen, South-Norway, during the "Little Ice Age" maximum. *The Cryosphere* **3**(2), 231–243. doi:10.5194/tc-3-231-2009

**Boyer D and Howe C** (2024) *Global Glacier Casualty List*. August 17, 2024 doi:10.25613/CZJA-9V56

**Burrill J, Dannevig H and Brendehaug E** (2025) What are melting glaciers good for? Examining the extent of glacier retreat on tourist engagement with climate change. *Scandinavian Journal of Hospitality and Tourism* 1–23. doi:10.1080/15022250.2025.2508711

**Cogley JG and 11 others** (2011) Glossary of glacier mass balance and related terms, IHP-VII Technical Documents in Hydrology No. 86. In *IACS Contribution, No. 2*. Paris: UNESCO-IHP, pp.114.

**Carrivick JL, James WH, Grimes M, Sutherland JL and Lorrey AM** (2020) Ice thickness and volume changes across the Southern Alps, New Zealand, from the little ice age to present. *Scientific Reports* **10**(1), 13392. doi:10.1038/s41598-020-70276-8

**Carrivick JL, Andreassen LM, Nesje A and Yde JC** (2022) A reconstruction of Jostedalsbreen during the Little Ice Age and geometric changes to outlet glaciers since then. *Quaternary Science Reviews* **284**, 107501.

**Ezzat L** and **19 others** (2025) Diversity and biogeography of the bacterial microbiome in glacier-fed streams. *Nature* **637**, 622–630. doi:10.1038/s41586-024-08313-z

**Grove JM** (2004) Little Ice Ages. Ancient and Modern. Volumes 1 and 2, 2nd edition. *Geological Magazine* **142**(3), 314–314.

**Huss M** (2013) Density assumptions for converting geodetic glacier volume change to mass change. *The Cryosphere* **7**, 877–887.

**Harsson BG and Aanrud R** (2016) *Med Kart Skal Landet Bygges. Oppmåling Og Kartlegging Av Norge 1773-2016*. Ringerike: Statens kartverk.

**Hugonnet R, Brun F, Berthier E, Dehecq A, Mannerfelt ES, Eckert N and Farinotti D** (2022) Uncertainty analysis of digital elevation models by spatial inference from stable terrain. *IEEE Journal of Selected Topics in Applied Earth Observations and Remote Sensing* **15**, 6456–6472.

**Hugonnet R and 15 others** (2024) *xDEM* (Version 0.1.0) [Computer software]. Zenodo. doi:10.5281/zenodo.11492983

**Howe C and Boyer D** (2025) Social impacts of glacier loss. *Science* **388**, 914–915. doi:10.1126/science.ady1688

**Johannessen F** (1928) Breifonn - Norges sydpol. *Stavanger Turistforening Årbok* **1928**, 148–155.

**James MR, Robson S and Smith MW** (2017) 3-D uncertainty-based topographic change detection with structure-from-motion photogrammetry: Precision maps for ground control and directly georeferenced surveys. *Earth Surface Processes and Landforms* **42**, 1769–1788.

**Liestøl O** (1962) List of the area and number of glaciers. In Hoel A and Werenskiold W (eds), *Glaciers and Snowfields in Norway, Norsk Polarinstitutt Skrifter*, Vol. 114 : Oslo University Press, Oslo, 35–54.

**Leigh JR and 5 others** (2019) Identifying and mapping very small (<0.5 km2) mountain glaciers on coarse to high-resolution imagery. *Journal of Glaciology* **65**(254), 873–888. doi:10.1017/jog.2019.50

**Lee E, Carrivick JL, Quincey DJ, Cook SJ, James WH and Brown LE** (2021) Accelerated mass loss of Himalayan glaciers since the Little Ice Age. *Scientific Reports* **11**(1), 24284. doi:10.1038/s41598-021-03805-8

**McNabb R, Nuth C, Kääb A and Girod L** (2019) Sensitivity of glacier volume change estimation to DEM void interpolation. *The Cryosphere* **13**(3), 895–910. doi:10.5194/tc-13-895-2019

**Naeser W** (1857) Rektangelmåling 12C 4; 12C 8; 12C 12; 12D 1; 12D 2; 12D 3; 12D 5; 12D 6; 12D 9; 12D 10 [Map; 1:100 000]

**Nussbaumer SU, Nesje A and Zumbühl HJ** (2011) Historical glacier fluctuations of Jostedalsbreen and Folgefonna (southern Norway) reassessed by new

pictorial and written evidence. *The Holocene* **21**(3), 455–471. doi:10.1177/0959683610385728

**Nuth C and Kääb A** (2011) Co-registration and bias corrections of satellite elevation data sets for quantifying glacier thickness change. *The Cryosphere* **5**, 271–290. doi:10.5194/tc-5-271-2011

**Østrem G and Ziegler T** (1969) Atlas over breer i Sør-Norge (Atlas of glaciers in South Norway). *NVE Meddelelse*, **20**. Hydrologisk avdeling, Norges Vassdrags- og Elektrisitetsvesen.

**Østrem G, Dale Selvig K and Tandberg K** (1988) Atlas over breer i Sør-Norge (Atlas of glaciers in South Norway). *NVE Meddelelse*, **61**. Hydrologisk avdeling, Norges Vassdrags- og Energiverk.

**Osipov EY and Osipova OP** (2019) Reconstruction of the Little Ice Age glaciers and equilibrium line altitudes in the Kodar Range, southeast Siberia. *Quaternary International* **524**, 102–114. doi:10.1016/j.quaint.2018.11.033

**Paul F and 10 others** (2013) On the accuracy of glacier outlines derived from remote-sensing data. *Annals of Glaciology* **54**(63), 171–182. doi:10.3189/2013AoG63A296

**Paul F, Andreassen LM and Winsvold SH** (2011) A new glacier inventory for the Jostedalsbreen region, Norway, from Landsat TM scenes of 2006 and changes since 1966. *Annals of Glaciology* **52**, 153–162.

**Purdie H** (2013) Glacier retreat and tourism: Insights from New Zealand. *Mountain Research and Development* **33**(4), 463–472. doi:10.1659/MRD-JOURNAL-D-12-00073.1

**Reinthaler J and Paul F** (2023) Using a web map service to map Little Ice Age glacier extents at regional scales. *Annals of Glaciology* **64**(92), 206–224. doi:10.1017/aog.2023.39

**Raup B, Andreassen LM, Boyer D, Howe C, Pelto M and Rabatel A** (2025) Tracking extinct glaciers in GLIMS. *Annals of Glaciology* **66**, 1–6. doi:10.1017/aog.2025.10027

**Scharffenberg HC** (1856) Rektangelmåling 12D 5; 12D 6; 12D 9; 12D 10 [Map; 1:50 000].

**Staib F** (1860) Portefølje nr 20 [Map; 1:100 000]. *Porteføljekart - Norge 166*.

**SeNorge** (2025) https://senorge.no/License (accessed March 2025).

**Sigmond EM** (1975) Geologisk kart over Norge, berggrunnskart SAUDA 1: 250 000. Norges geologiske undersøkelse.

**Smith MW, Carrivick JL and Quincey DJ** (2016) Structure from motion photogrammetry in physical geography. *Progress in Physical Geography* **40**(2), 247–275.

**Stokes CR, Andreassen LM, Champion MR and Corner GD** (2018) Widespread and accelerating glacier retreat on the Lyngen Peninsula, northern Norway, since their 'Little Ice Age' maximum. *Journal of Glaciology* **64**(243), 100–118. doi:10.1017/jog.2018.3

**Tvede AM** (1973) Folgefonni – En glasiologisk avviker. *Naturen* **97**, 11–16.

**Tielidze LG, Mackintosh AN, Gavashelishvili A, Gadrani L, Nadaraia A and Elashvili M** (2025) Post-Little Ice Age Equilibrium-Line Altitude and Temperature Changes in the Greater Caucasus Based on Small Glaciers. *Remote Sensing* **17**(9), 1486. doi:10.3390/rs17091486

**Wareberg G** (1927) Til tops. *Stavanger Turistforening Årbok* **1927**, 24–32.

**Winsvold SH, Andreassen LM and Kienholz C** (2014) Glacier area and length changes in Norway from repeat inventories. *The Cryosphere* **8**, 1885–1903. doi:10.5194/tc-8-1885-2014

**Weber P, Boston CM, Lovell H and Andreassen LM** (2019) Evolution of the Norwegian plateau icefield Hardangerjøkulen since the 'Little Ice Age'. *The Holocene* **29**(12), 1885–1905.

**Weber P, Lovell H, Andreassen LM and Boston C** (2020) Reconstructing the Little Ice Age extent of Langfjordjøkelen, Arctic mainland Norway, as a baseline for assessing Centennial-scale icefield recession. *Polar Research* **39**, 4304.

**Zhang H, Xu X, Sun Y, Li J and Xu B** (2024) Reconstructions of Little Ice Age glaciers and climate in the Tanggula Mountains, central Tibet Plateau. *Palaeogeography, Palaeoclimatology, Palaeoecology* **637**, 112008. doi:10.1016/j.palaeo.2023.112008

**Zekollari H** and **20 others** (2025) Glacier preservation doubled by limiting warming to 1.5°C versus 2.7°C. *Science* **388**, 979–983. doi:10.1126/science.adu4675

https://doi.org/10.1017/aog.2025.10029 Published online by Cambridge University Press